

Article

Advances in Engine Efficiency: Nanomaterials, Surface Engineering, and Quantum-Based Propulsion

Mario J. Pinheiro 

Department of Physics, Instituto Superior Técnico—IST, Universidade de Lisboa—UL, Av. Rovisco Pais, 1049-001 Lisboa, Portugal; mpinheiro@tecnico.ulisboa.pt

Abstract: This study explores ground-breaking methods for improving engine efficiency by combining cutting-edge materials, theoretical frameworks, and alternative energy paradigms. The paper primarily offers a cohesive framework, built from our variational method which combines thermal and entropic engines. We investigate the fabrication of hydrophobic and other functionally specific surfaces using nanomaterials and sophisticated surface engineering techniques that efficiently utilize entropy gradient forces. Additionally, this publication explores the fields of quantum-based propulsion systems and information-burning engines, creating a connecting link between theoretical foundations and real-world technical implementations. The study emphasizes the multifaceted character of engine research and its crucial role in shaping a future in which sustainability and efficiency are intimately connected.

Keywords: thermodynamics; energy conversion; nonlinear dynamics and chaos; renewable energy; information-burning engines; propulsion

1. Introduction

Engines are crucial devices in modern society, providing power to everything from vehicles to generators. However, the efficiency of these engines is fundamentally limited by the laws of thermodynamics, which dictate that only a portion of the available energy can be converted into useful work. To overcome these limitations and improve engine efficiency, researchers are exploring innovative materials and design concepts that can better harness available energy sources.

One promising area of research is the use of nanomaterials and surface engineering to create hydrophobic surfaces that can harness entropy gradient forces to generate useful work. These surfaces are capable of converting the random thermal motion of water molecules into directed motion, which can be used to perform work [1,2]. Another area of intense research is the development of information-burning engines, which operate by extracting energy from information processing, rather than from traditional thermal or chemical energy sources. This approach is inspired by the theoretical foundations laid by Maxwell's demon, illustrating how information can be used to extract work from a thermodynamic system [3–6].

The exploration of quantum thermodynamics has opened new avenues for energy conversion and utilization. Quantum engines, particularly those based on the Otto and Stirling cycles, have shown the potential to exceed classical efficiency limits under certain conditions [5,6]. These engines exploit quantum mechanical effects, such as coherence and entanglement, to improve their performance [7,8].

In this context, the fundamental equation of dynamics can be expressed in various forms to analyze different types of engines. For thermal engine analysis, it can be written as:

$$m\vec{a} = \vec{F}^{ext} + \frac{\partial}{\partial \vec{r}}(TS). \quad (1)$$



Citation: Pinheiro, M.J. Advances in Engine Efficiency: Nanomaterials, Surface Engineering, and Quantum-Based Propulsion. *Magnetochemistry* **2024**, *10*, 17. <https://doi.org/10.3390/magnetochemistry10030017>

Academic Editor: Adriana Greco

Received: 29 December 2023

Revised: 19 February 2024

Accepted: 23 February 2024

Published: 27 February 2024



Copyright: © 2024 by the authors. Licensee MDPI, Basel, Switzerland. This article is an open access article distributed under the terms and conditions of the Creative Commons Attribution (CC BY) license (<https://creativecommons.org/licenses/by/4.0/>).

When considering systems subject to a potential field, the equation takes the form:

$$\frac{d\mathbf{p}}{dt} = -\nabla V^{ext} + \nabla \left(T \sum_i \rho_i \ln \rho_i \right) \quad (2)$$

for information-burning engines, with

$$\rho_i = \frac{n_i}{N}, \quad (3)$$

where n_i refers to the energy-dependent probabilities of various alternative microstates, and ρ_i represents the energy-dependent probabilities of different alternative microstates in the information-burning engines. In the context of understanding the dynamics of a particular system subject to both external potentials and internal thermodynamic drives, it may be seen as an advantage in the present formulation of the equation of motion.

Analyzing the forces involved, the first term, $-\nabla V^{ext}$, represents the force due to the external potential, predominantly exploited in our mechanized society to sustain the momentum of machinery and technological processes; while the second term, $\nabla (T \sum_i \rho_i \ln \rho_i)$, can be perceived as an entropic force, establishing a connection between thermodynamic concepts and the equation of motion. Notably, the gradient in the entropic term implies a drive towards the maximization of entropy in scenarios devoid of other prevailing forces.

Of course, Equation (2) is still a classical dynamic equation. The passage from a dynamical equation (Equation (1)) to a quantum mechanical-like equation, integrating thermodynamic and informational aspects, is quite a unique and complex development. In the derivation of the Schrödinger-like equation from the dynamical equation (Equation (1)), we leverage the canonical quantization, a procedure that provides a bridge between classical physics and quantum mechanics, substituting $p \rightarrow i\hbar\nabla$ and $E \equiv H = i\hbar\partial_t$. In the context provided, considering the novel term (\mathcal{J}) that incorporates some form of entropic or informational contribution leads us directly to an entropy-modified quantum dynamics (EMQD), denoting an entropic modification to standard quantum dynamics, and the novel contribution of this work. Let us summarize the provided equation. Consider the wave function $\Psi(\mathbf{r}, t)$. The Hamiltonian of the system is denoted by H , and V represents the usual external potential. The term \mathcal{J} may be an expression that incorporates the thermomechanical and/or informational components of the system. The proposed quantum mechanical-like equation can be written as (see, e.g., Ref. [9] for more details in applications to dynamics, and Ref. [10] for applications in econophysics):

$$H\Psi = i\hbar \frac{\partial\Psi}{\partial t} = -\frac{\hbar^2}{2m} \nabla^2\Psi + V\Psi + \mathcal{J}\Psi, \quad (4)$$

where:

- $\Psi(\mathbf{r}, t)$: wavefunction of the stock price S at a given instant of time t .
- \hbar : reduced Planck's constant.
- m : mass of the particle.
- V : external potential.
- $\mathcal{J} \equiv \frac{I^2}{2I} - (\boldsymbol{\omega} \cdot \mathbf{J}) - \Delta F$: a term that might involve thermomechanical and/or informational aspects, with \mathbf{J} denoting the total sum of orbital and spin angular momentum, I the moment of inertia, $\boldsymbol{\omega}$ the instantaneous angular velocity of the system, and ΔF the free energy function.

The development of more efficient engines is a critical goal for both environmental and economic reasons, as reducing energy waste can help mitigate climate change and improve energy security. Advances in materials science, engineering, and thermodynamics are all contributing to this effort, and there is reason to be optimistic about the potential for new and innovative engine designs in the future.

The search for more effective engines is, in general, a multidisciplinary endeavor that necessitates cooperation between scientists and engineers from numerous domains. Engine

technology has the ability to drastically minimize energy waste and open the door to a more sustainable future study and innovation.

As we move towards a more data-driven society, the ability to harness energy from information processing could become increasingly important. Information-burning engines offer a viable path towards more sustainable and effective energy production. They may also open up new possibilities for applications in AI and quantum computing. This is the motivation of the present work, which aims to investigate the potential of information-burning engines and advance our understanding of their underlying principles and design concepts. We seek to contribute to the development of more effective and sustainable engines, as well as open the way for creative applications in emerging technologies by investigating new methods for transforming information into useful work.

In this paper, we explore advances in engine efficiency through the integration of nanomaterials, surface engineering, quantum-based propulsion, and information-burning engines. Section 1.1 delves into the fabrication and utilization of hydrophobic surfaces and other nanomaterials for efficiently harnessing entropy gradient forces. Section 1.2 investigates the conceptual framework and potential of information-burning engines, highlighting their unique energy extraction mechanisms. Section 1.3 discusses the theoretical underpinnings and advantages of engines fueled by quantum entanglement, emphasizing its efficiency and experimental realizations. Section 1.5 presents an innovative approach to propulsion using metamaterials, exploring the theoretical and experimental advancements that enable the generation of thrust through electromagnetic interactions. The conclusion in Section 2 synthesizes the insights gained from these diverse methodologies, underscoring the multidisciplinary effort required to push the boundaries of engine efficiency and sustainability.

1.1. Thermal Engines

The articulated framework presented in Equation (1), while rooted in acknowledged thermodynamic precepts, prominently advocates an integrated approach that seamlessly bridges thermal and quantum/information engines. This is expressed explicitly through the relation,

$$\Delta W_{irr} = \int_i^f m(\vec{a} \cdot d\vec{r}) = T_0 \sum \Delta S, \quad (5)$$

where ΔW_{irr} represents the genuine decrement in work W due to irreversibility, T_0 is the temperature of the medium, and $\sum \Delta S$ signifies the augmentation of the total entropy of the fluid and the heat source.

Emphasizing further, Equation (1) is not merely a restatement of known thermodynamic relationships but serves as an integrated analytical framework, combining classical thermodynamic principles with quantum and information mechanical systems. This confluence of classical and quantum perspectives offered by Equation (1) promises to be a robust tool for analyzing and interpreting phenomena where quantum and thermodynamic effects are mutually entangled. Thus, through an adroit application of this integrated approach, novel insights and potentially revolutionary understandings of intricate thermodynamic and quantum systems can be harvested, especially in scenarios where quantum effects are non-negligible and intersect with classical thermodynamic behaviors.

To use the quantum version of the dynamical equation of motion given by Equation (1) to calculate the thrust of the Stirling quantum engine, we need to express the external force \vec{F}^{ext} and the entropy S as quantum mechanical operators.

Assuming that the external force is constant and acts along the x-axis, we can express it as $\vec{F}^{ext} = F^{ext} \hat{x}$, where F^{ext} is a constant and \hat{x} is the position operator along the x-axis. The entropy operator can be written as $\hat{S} = -k_B \ln(\hat{\rho})$, where k_B is the Boltzmann constant and $\hat{\rho}$ is the density operator of the system.

To address a possible mechanism of interest, for example, to obtain the equation for the thrust of the Otto quantum engine [11], we need to determine the time evolution of the

density operator $\hat{\rho}$ (see again Section 1). This can be done using the von Neumann equation:

$$i\hbar \frac{\partial \hat{\rho}}{\partial t} = [\hat{H}, \hat{\rho}], \quad (6)$$

where \hat{H} is the Hamiltonian of the system. The Hamiltonian of the Otto quantum engine can be written as:

$$\hat{H} = \frac{\hat{p}^2}{2m} + V(\hat{x}) + \mathcal{J}, \quad (7)$$

where \hat{p} is the momentum operator, m is the mass of the engine, and $V(\hat{x})$ is the potential energy of the engine as a function of position, and \mathcal{J} represents thermo-mechanical and/or informational aspects.

Using Equations (6) and (7), we can calculate the time evolution of the position operator \hat{x} , which can then be used to determine the thrust of the engine. However, calculating the thrust of the Otto quantum engine using this approach can be quite challenging.

1.2. Information-Burned Engine

The information-driven engine is rooted in the Maxwell-demon Gedankenexperiment. Quantum thermodynamics is a rapidly growing field, and Ref. [12] provides an extensive overview of the principles and applications of quantum thermodynamic processes and offers insights into the future of energy conversion and information processing.

To analyze the working mechanism of this engine, we ought to choose to write the classical macroscopic equation under the form:

$$m\vec{a} = \vec{F}^{ext} + \frac{\partial}{\partial \vec{r}} \left(T \sum_i \rho_i \ln \rho_i \right). \quad (8)$$

Considering that $F = -kT \ln e^{-\beta E_0}$, it can be inferred that the maximal power output of this engine is given by

$$P_{max} = \frac{E_0}{\tau}, \quad (9)$$

where E_0 is the minimal energy (eigenvalue of the Hamiltonian) at the disposal of the system in a given time τ , assuming the medium temperature is low enough, $T_0 \rightarrow 0$. For example, Tushar K. Saha et al. [13] demonstrated that a heavy colloidal particle held by an optical trap and immersed in water can be lifted against gravity via a ratchet mechanism, achieving a maximal power output estimated to be $10^3 \frac{kT}{s}$ and a maximum velocity of $190 \mu\text{m/s}$.

The definition of entropy as an operator in the context of quantum thermodynamics is essential to grasping the microscopic underpinnings of thermodynamic processes. This idea, which has its roots in ensemble theory, posits that entropy can be written as $S = -k_B \langle \ln \rho \rangle$, in which ρ represents the density matrix of the system and k_B stands for the Boltzmann constant. This formulation provides a quantum statistical interpretation of entropy, in line with the seminal contributions of John von Neumann to the fields of thermodynamics and quantum mechanics [14]. Moreover, Greiner et al.'s [15] extensive work from 1995 explores ensemble theory and offers a thorough explanation of statistical thermodynamics and the quantum-mechanical foundations for it. Additional references can be obtained in Refs. [16,17].

An integrated network of sensors and actuators, adept at identifying and responding to the microstates of the surrounding environment, may be utilized within an information-driven mechanism to mobilize a meso-apparatus, as opposed to a heavy colloidal particle, in accordance with the methodology proposed by Equation (8). The probability density function ρ would be used to describe the likelihood that the meso-apparatus would be in a specific microstate ρ_i , depending on factors like the location and speed of other moving bodies on the road, the slope of the road, and so on. These data would allow the system to predict the meso-apparatus's most likely future microstate and modify the vehicle's

speed and direction accordingly. For example, the system could slow down the device before a stoppage if it considers that there is a greater likelihood that the vehicle will face collisions ahead. In examining the microstate probabilities and choosing the optimum course of action, a sophisticated algorithm would be needed, but the procedure would improve driving efficiency and safety if correctly applied.

1.3. Engine Fueled by Entanglement

An interesting investigation into the application of quantum mechanical principles to thermal machines is presented by introducing the focus on quantum Stirling engines within the field of quantum thermodynamics. The quantum Stirling engine offers a compelling advantage by combining isothermal processes along with adiabatic transitions, in contrast to the quantum Otto engine, which functions through adiabatic compression and expansion processes paired with isochoric heating and cooling. This differentiation is important because the Stirling cycle's intrinsic isothermal processes enable direct heat exchange with reservoirs at constant temperatures, which may improve engine efficiency by utilising quantum coherence and entanglement in a way that is specific to the quantum domain. Therefore, studying the interface between quantum mechanics and classical thermodynamic cycles with the quantum Stirling engine presents a strong possibility for advances in quantum heat management, energy conversion, and the creation of quantum thermal devices [18–21].

In order to lay the groundwork for a thorough analysis of the quantum Stirling engine's capabilities and the pursuit of novel directions in quantum engine research, this section will examine the operational principles, theoretical foundations, and possible benefits of the engine [5,6,22].

The efficiency of this cycle, which depends on the temperatures of the heat reservoirs and the compression ratio of the quantum states, as well as its successful experimental realizations in systems such as trapped ions and quantum dots, highlight its potential superiority and practical viability. However, the decision between Otto and Stirling cycles ultimately depends on the particular quantum system and application; current research examines the advantages and disadvantages of each cycle in the quantum domain and, in particular, we now focus on the Stirling cycle.

Equation (8) was initially intended to represent a classical system. It would be necessary to make significant changes to the original equation to adapt it to describe a quantum Stirling engine. However, there is great potential for engines fueled by entanglement, a quantum-mechanical phenomenon in which two particles become linked in such a way that the state of one particle is dependent on the state of the other, regardless of the distance between them. In these engines, entangled particles are used to extract work from heat baths, and the process is driven by a violation of local realism, a fundamental assumption in classical physics. The exploration of quantum thermodynamics and the potential of quantum coherence engines has been significantly advanced by recent works such as Park et al. (2013) [23] and Ozdemir and Müstecaplıolu (2020) [24], which highlight the innovative use of quantum information to drive heat engines and the exploration of quantum coherence in operational engines. These theoretical frameworks extend the concept of traditional heat engines into the quantum realm, offering new insights into the role of quantum entanglement and coherence in energy conversion processes. Several theoretical proposals have been made for these engines, beginning with a three-level maser as a heat engine [25] that already offers a comprehensive exploration of system dynamics, dealing with energy transitions, thermal contact, and energy exchange between different thermal reservoirs, until more recently including a quantum Otto engine [26,27] and a quantum refrigerator [28,29].

In summary, the engine is made up of two subsystems A and B that are entangled, meaning that they are in a quantum state where the properties of one subsystem are correlated with the properties of the other subsystem. The first subsystem, which we will call the “information engine”, is responsible for processing information and converting

it into work. The second subsystem, which we will call the “thermal bath”, is a reservoir of heat that is in contact with the information engine and provides the energy needed to perform work. The entangled state of two particles can be written as:

$$|\psi\rangle = \frac{1}{\sqrt{2}}(|0\rangle_A|1\rangle_B - |1\rangle_A|0\rangle_B). \quad (10)$$

Here, $|0\rangle$ and $|1\rangle$ represent the two possible states of a qubit, and A and B represent the two subsystems. The work performed by the information engine in the time interval from instant t_1 to t_2 can be written in terms of the Hamiltonian operator \hat{H} and the wave function ψ :

$$W = \int_{t_1}^{t_2} \langle \psi | \frac{d\hat{H}}{dt} | \psi \rangle dt. \quad (11)$$

The thermal bath is modeled as a collection of harmonic oscillators, and its state is described by the density operator $\hat{\rho}$:

$$\hat{\rho} = \frac{e^{-\beta\hat{H}}}{\text{Tr}e^{-\beta\hat{H}}}, \quad (12)$$

where β is the inverse temperature of the bath.

The quantum Stirling engine is based on the cyclic operation of four steps ($i = 1, \dots, 4$), described by the following unitary operators:

$$\hat{U}_i = e^{-i\hat{H}_i\tau_i/\hbar}, \quad (13)$$

where \hat{H}_i is the Hamiltonian of the engine during the i -th step, and τ_i is the duration of the i -th step. The quantum Stirling engine involves the following four steps:

1. Isothermal expansion: during this step, the engine is coupled to a hot thermal reservoir at temperature T_H and expands isothermally while doing work. The unitary transformation associated with this step is $\hat{U}_1 = e^{-i\hat{H}_1\tau_1/\hbar}$, where \hat{H}_1 is the Hamiltonian of the engine during this step.
2. Adiabatic expansion: during this step, the engine is thermally isolated and expands adiabatically while doing work. The unitary transformation associated with this step is $\hat{U}_2 = e^{-i\hat{H}_2\tau_2/\hbar}$, where \hat{H}_2 is the Hamiltonian of the engine during this step.
3. Isothermal compression: during this step, the engine is coupled to a cold thermal reservoir at temperature T_C and isothermally compresses while working on it. The unitary transformation associated with this step is $\hat{U}_3 = e^{-i\hat{H}_3\tau_3/\hbar}$, where \hat{H}_3 is the Hamiltonian of the engine during this step.
4. Adiabatic compression: during this step, the engine is thermally isolated and compresses adiabatically while work is carried out. The unitary transformation associated with this step is $\hat{U}_4 = e^{-i\hat{H}_4\tau_4/\hbar}$, where \hat{H}_4 is the Hamiltonian of the engine during this step.

The engine architecture and the thermodynamic cycle that are used determine the precise shape of the Hamiltonians and the lengths of the steps. Therefore, to determine the work and thrust, we must first define the Hamiltonians $\hat{H}_1, \hat{H}_2, \hat{H}_3$, and \hat{H}_4 . Let us suppose that the system is a straightforward two-level system qubit. The Hamiltonians at each stage are expressed as follows:

$$\hat{H}_i = \omega_i|1\rangle\langle 1|, \quad (14)$$

where ω_i denotes the energy difference between the qubit's two states at step i ($i = 1, \dots, 4$). The derivative of each Hamiltonian for time can be determined as ($i = 1, \dots, 4$):

$$\frac{d\hat{H}_i}{dt} = \frac{d\omega_i}{dt}|1\rangle\langle 1|. \quad (15)$$

Now that the integral of each derivative has been evaluated, the work carried out during each step can be calculated, assuming that each step takes τ_1 , τ_2 , τ_3 , and τ_4 time. At each stage ($i = 1, \dots, 4$), they are as follows:

$$W_i = \int_0^{\tau_i} \langle \psi | \frac{d\hat{H}_i}{dt} | \psi \rangle dt. \quad (16)$$

For a complete cycle, the total work performed is the sum of the work performed during each step.

$$W_{\text{total}} = \sum_{i=1}^4 W_i. \quad (17)$$

Next, we can calculate the thrust T using the following relationship:

$$T = \frac{\sum_{i=1}^4 F_i \tau_i}{T_{\text{cycle}}}, \quad (18)$$

where F_i is the force exerted during the cycle, τ_i is the duration of step i , and T_{cycle} is the total time taken for the engine to complete a cycle.

With more qubits present in the system, the quantum Stirling engine creates more thrust. We are still a long way from realizing the notion in practice. To boost the efficiency of a quantum Stirling engine, a material or element should have the following qualities: (i) stable energy levels (in order to properly regulate and control the quantum processes required for the engine cycle, the material must contain consistently stable, clearly defined energy levels); (ii) coherent interactions (to maintain quantum coherence throughout the engine cycle, even when connected to thermal reservoirs, the substance must exhibit coherent interactions between its component particles, such as qubits); (iii) efficient heat dissipation (to maintain the optimum operating conditions during the isothermal phases of the engine cycle, the material must allow efficient heat dissipation); (iv) scalability (the material must allow the installation of a high number of qubits to boost the thrust and overall performance of the quantum Stirling engine.)

The key to making the device move on an information budget is to make use of the intimate linkages between quantum information and thermodynamics. In particular, it has been shown that the amount of work that can be extracted from a system is constrained by the amount of information that can be acquired about it without disturbing it. This concept may be used, for instance, by building the information engine so that it extracts work by “measuring” the degree of entanglement between the two subsystems. By carefully adjusting the measurements, it is possible to “squeeze” energy out of the correlations between the two subsystems and obtain energy from the entanglement without disrupting the quantum state. The mathematical equations that describe this process vary in complexity depending on the specifics of the system under study. The core idea is that the entanglement between the two subsystems allows for the flow of energy and information that may be used to perform work even in the absence of a direct source of energy like fuel or electricity.

One possible set of equations that can be used to describe this process is based on the concept of quantum mutual information. The mutual information between two quantum subsystems, denoted as A and B , is defined as: $H(A : B) = H(A) + H(B) - H(AB)$ or, equivalently, $I(A : B) = S_A + S_B - S_{AB}$, where S_A , S_B , and S_{AB} are the von Neumann entropies of subsystem A , subsystem B , and joint subsystem AB , respectively. Using these concepts, it is possible to derive the maximum amount of work that can be extracted from the entangled subsystems A and B as:

$$\Delta S = \frac{\Delta Q}{T}, \quad (19)$$

$$I(A : B) = S_A + S_B - S_{AB}, \quad (20)$$

$$S = -\text{tr}(\rho \log \rho), \quad (21)$$

and

$$W_{\max} = k_B T \Delta I(A : B), \quad (22)$$

with T denoting the temperature of the thermal bath, and $\Delta I(A : B)$ is the change in mutual information between subsystems A and B during the work extraction process.

An example of an information engine is the Brownian ratchet, which operates using the random motion of particles in a fluid. The ratchet consists of a series of asymmetric barriers, which allow particles to move in one direction but not the other. The basic idea of the Brownian ratchet can be described by the following equation:

$$W = k_B T \ln \left(\frac{p_f}{p_i} \right), \quad (23)$$

where W is the work performed by the ratchet, T is the temperature, p_f is the probability of the ratchet moving forward, and p_i is the probability of it moving backward. The probability of the ratchet moving forward can be increased by “information ratcheting”, which involves using information about the particles’ positions to manipulate the barriers. One way to do this is to use a series of sensors to measure the positions of the particles and then use this information to control the barriers. The amount of work the ratchet does can be used to calculate the thrust generated by the device. For a Brownian ratchet, the maximum efficiency is given by the Carnot limit, which is $\eta_{\max} = 1 - \frac{T_L}{T_H}$, where T_L is the temperature of the environment and T_H is the temperature of the heat source. This equation allows us to calculate the maximum thrust of the ratchet. The precise ratchet design and the effectiveness of the information ratcheting mechanism will determine the thrust.

One proposal for achieving this involves using a process called “quantum squeezing”, in which the fluctuations of certain quantum observables are reduced below their usual quantum limits [30,31].

Hence, first, we will calculate the von Neumann entropy for the quantum Stirling engine at each step of the cycle and, for its use, we need the density matrix at different stages of the Stirling cycle. Applying the corresponding unitary transformations to the initial density matrix ρ_0 ($i = 1, \dots, 4$):

$$\rho_i = \hat{U}_i \rho_0 \hat{U}_i^\dagger. \quad (24)$$

After obtaining the density matrices for each step, you can calculate the von Neumann entropy at each step ($i = 1, \dots, 4$):

$$S_i = -\text{Tr}(\rho_i \log_2 \rho_i). \quad (25)$$

To calculate the work performed during each step of the quantum Stirling cycle, we can use the following relation

$$W_i = \Delta E_i = E_i - E_{i-1}, \quad (26)$$

where W_i is the work carried out during step i , and ΔE_i is the change in the engine energy during step i . The energy of the engine can be found using the expectation value of the Hamiltonian:

$$E_i = \text{Tr}(\rho_i \hat{H}_i). \quad (27)$$

Finally, to calculate the total work performed during the quantum Stirling cycle, sum the work carried out during each step:

$$W_{\text{total}} = W_1 + W_2 + W_3 + W_4. \quad (28)$$

The thrust generated by the Stirling quantum engine can be estimated by dividing the total work performed by the cycle duration:

$$T = \frac{W_{\text{total}}}{\tau_{\text{total}}}, \quad (29)$$

where τ_{total} is the total duration of the quantum Stirling cycle, given by:

$$\tau_{\text{total}} = \tau_1 + \tau_2 + \tau_3 + \tau_4. \quad (30)$$

To estimate the thrust in Newtons, we need to have more realistic values for the work carried out during each step and the durations of each step. Additionally, we need to convert the total work performed during the quantum Stirling cycle to force and relate it to the thrust. Here, we will provide an example calculation based on some assumptions. Assume the following work is completed at each step: $W_1 = 1 \times 10^{-23}$ J, $W_2 = 0.8 \times 10^{-23}$ J, $W_3 = -0.6 \times 10^{-23}$ J, $W_4 = -0.5 \times 10^{-23}$ J, and let the durations of each step be corresponding $\tau_1 = 10^{-6}$ s, $\tau_2 = 2 \times 10^{-6}$ s, $\tau_3 = 10^{-6}$ s, $\tau_4 = 2 \times 10^{-6}$ s; those values are assumptions, simplifications made for the purpose of the calculation.

The sum of the work performed during each step gives the total work carried out during the quantum Stirling cycle:

$$W_{\text{total}} = W_1 + W_2 + W_3 + W_4 = 0.7 \times 10^{-23} \text{ J}. \quad (31)$$

The total duration of the cycle is:

$$\tau_{\text{total}} = \tau_1 + \tau_2 + \tau_3 + \tau_4 = 6 \times 10^{-6} \text{ s}. \quad (32)$$

Next, let us assume the quantum engine moves over a distance d during the Stirling cycle. The average force F acting on the engine can be calculated as:

$$F = \frac{W_{\text{total}}}{d}. \quad (33)$$

Assuming that the engine moves over a very small distance, for instance, $d = 10^{-9}$ m (1 nanometer), we can estimate the average force:

$$F = \frac{0.7 \times 10^{-23} \text{ J}}{10^{-9} \text{ m}} = 7 \times 10^{-15} \text{ N}. \quad (34)$$

This estimate assumes a 1-qubit Stirling quantum engine with specific values for the work carried out during each step and the step durations. However, we will now scale the system with the number of qubits N in the ion trap. The complexity of the system grows exponentially with the number of qubits N . However, since the qubits are assumed to be non-interacting and independent, the total work performed during the cycle should scale linearly with the number of qubits. For a system with N qubits (see Ref. [31]), the total work carried out during the quantum Stirling cycle can be approximated as:

$$W_{\text{total}}(N) = N \times W_{\text{total}}(1). \quad (35)$$

Here, $W_{\text{total}}(1)$ is the total work performed for the 1-qubit Stirling quantum engine calculated earlier, which was 0.7×10^{-23} J. To estimate the average thrust for an N -qubit system, we can assume that the total duration of the cycle and the distance over which the engine moves remain unchanged. The average force and thrust can therefore be computed as follows:

$$F(N) = \frac{W_{\text{total}}(N)}{d} = N \times \frac{W_{\text{total}}(1)}{d}, \quad (36)$$

or

$$F(N) = N \times 7 \times 10^{-15} \text{ N}. \quad (37)$$

Here, $F(1)$ is the average force (or thrust) for the 1-qubit Stirling quantum engine calculated earlier, which is 7×10^{-15} N.

Although this might seem tiny at present, it is anticipated that, as technology develops and researchers seek to scale up ion-trap quantum computers, the number of qubits will increase. However, given the fast advancement of quantum computing technology and the appearance of competing strategies like superconducting qubits or topological qubits, forecasting the precise value of N in the future is challenging. Assuming linear scaling with the number of qubits and no major interactions or mistakes between qubits, this calculation provides an average thrust. Since there are various difficulties in increasing the number of qubits while keeping high fidelity, and since the linear scaling assumption may not hold for larger systems, the estimation fails to accurately reflect the performance of a quantum Stirling engine in real-world applications. Additionally, the scaling behavior and effectiveness of the quantum Stirling engine may be impacted by elements like decoherence, defective gates, and interactions between qubits. Though quantum technology, such as quantum computing, will depend on evolution and validation in propulsion applications, quantum Stirling engines may be expected to be used as CubeSat thrusters in the future.

1.4. The Stirling Engine

We now provide an analysis of the dynamics of a three-level maser system, including computations of various quantum mechanical properties like the density matrix evolution, work performed, entropy change. This is a clear example of how a quantum system can be modeled using a thermodynamic cycle analogous to classical thermodynamics, although it combines quantum mechanics, thermodynamics, and open system dynamics to describe a quantum version of the Stirling cycle.

In the quantum Stirling cycle, entropy changes are inherent to the isothermal processes where the system exchanges heat with external reservoirs at constant volume, distinct from its classical counterpart, which emphasizes adiabatic and isobaric transitions. Unlike classical thermodynamics, where entropy changes during isothermal expansions or compressions are more apparent, in quantum thermodynamics, these changes are crucially linked to quantum state transitions and interactions with heat baths. Specifically, during the isothermal heating and cooling phases of the quantum Stirling cycle, the system's entropy varies due to the absorption or release of heat, reflecting the transition between quantum states and the resultant statistical redistribution of populations among these states. This work delineates the mechanism of entropy variation within the cycle, underpinning the role of quantum state transitions and heat exchange in driving these changes. This quantitative analysis, rooted in quantum statistical mechanics, underscores the nuanced interplay between quantum coherence, entanglement, and thermalization processes, which collectively influence the cycle's thermodynamic efficiency.

1.4.1. System Parameters and Constants

The system under investigation is a three-level maser, see Figure 1. Although the foundational concept and the underlying mechanics are inspired by the previously described maser system [25], it should be noted that the exact parameter values used in our analysis were introduced independently. This allows for a broader investigation and the possibility of uncovering varied dynamical behaviors.

$$\omega_{12} = 1.50 \times 10^{11} \text{ rad/s}$$

$$\omega_{13} = 1.65 \times 10^{11} \text{ rad/s}$$

$$\omega_{23} = \omega_{13} - \omega_{12}.$$

1.4.2. Equations Used

The time evolution of the density matrix ρ under a Hamiltonian H is governed by the Liouville–von Neumann equation:

$$\frac{d\rho}{dt} = -\frac{i}{\hbar}[H, \rho]. \quad (38)$$

The quantum work carried out during a transition from ρ_{initial} to ρ_{final} under a Hamiltonian H is given by:

$$W = \hbar(\text{Tr}(H\rho_{\text{final}}) - \text{Tr}(H\rho_{\text{initial}})). \quad (39)$$

The von Neumann entropy of a quantum state ρ is given by:

$$S(\rho) = -\text{Tr}(\rho \log_2 \rho). \quad (40)$$

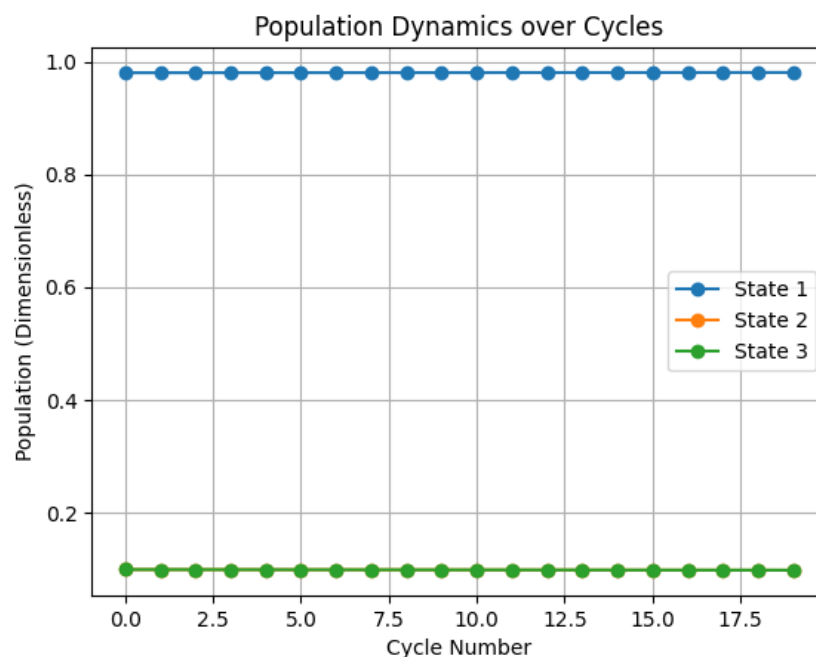


Figure 1. Evolution of state populations over multiple cycles in the quantum Stirling cycle. The dynamics indicate a preference towards populating the first energy level as cycles progress.

1.4.3. Results

After simulating the dynamics, we obtained the following results:

- Number of energy values: 4;
- Work per cycle: 0.2425994873046875 J;
- Power: 60,649,871.82617187 W;
- Entropy change per cycle: $6.92314106394308 \times 10^{-6}$ J/K.

This analysis provides a comprehensive understanding of the dynamics of a three-level maser system. The computed results can be used for further studies and optimizations related to quantum systems. The simulator code utilized for this analysis can be found on GitHub [32].

1.4.4. Quantum Stirling Engine: Entropy Dynamics

In our investigation of the quantum Stirling cycle, a notable observation was the consistent increase in the von Neumann entropy across successive cycles. This increase is indicative of the system evolving into a more mixed state over time. Under the influence of Lindblad superoperators in the model, this behavior can be attributed to the decoherence and dissipation effects that are introduced. In thermodynamics, this is akin to a nonideal or nonreversible process, where the system is gradually losing coherence. This rising entropy suggests that our quantum Stirling cycle, as captured in the current simulation, is not perfectly cyclic. External factors, primarily decoherence, nudge the system progressively away from its starting state with each cycle. Such deviations from a perfectly cyclic behavior intimate that, in practical applications of this quantum Stirling cycle, energy losses or inefficiencies might arise. Over extended cycles, the cumulative effect of these

inefficiencies could potentially lead to the decreased performance of the quantum heat engine; see Figures 2 and 3.

The von Neumann entropy is, after each cycle, a feature that is indicative of the system becoming more mixed (less pure) with each cycle, as shown in Table 1. By means of the Lindblad superoperators in the model, decoherence or dissipation is introduced, which leads to the quantum state becoming more mixed over time. In thermodynamic terms, this is a nonideal or nonreversible process, causing the system to lose coherence. The increase in the von Neumann entropy is consistent with an increase in the mixedness of the quantum state. A pure quantum state would have zero entropy, whereas a maximally mixed state would have maximum entropy. As decoherence and other processes progress, the system becomes more mixed, leading to the observed increase in entropy. Also, the increasing entropy suggests that the quantum Stirling cycle, as modeled in this simulation, is not perfectly cyclic. Instead, it is influenced by external factors such as decoherence that push the system away from its initial state with each cycle. The deviation from a perfectly cyclic behavior indicates that, in a real-world application of this quantum Stirling cycle, there would be energy losses or inefficiencies. Over multiple cycles, these inefficiencies accumulate, which might lead to a decreased performance of the quantum heat engine.

Table 1. Evolution of von Neumann entropy over cycles.

B	Von Neumann Entropy
1	6.28×10^{-6}
2	1.75×10^{-5}
3	2.54×10^{-5}
4	3.57×10^{-5}

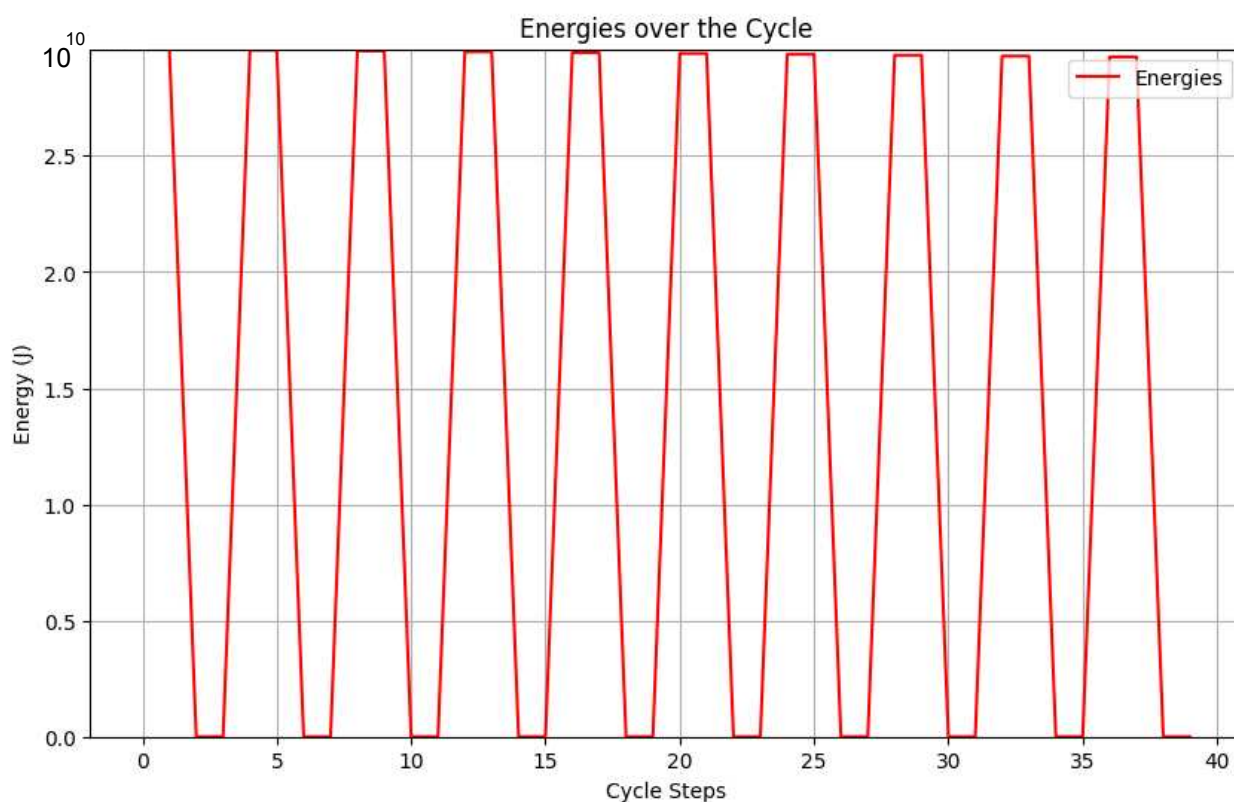


Figure 2. Energy dynamics of the quantum Stirling cycles, highlighting the periodic behaviors of each cycle.

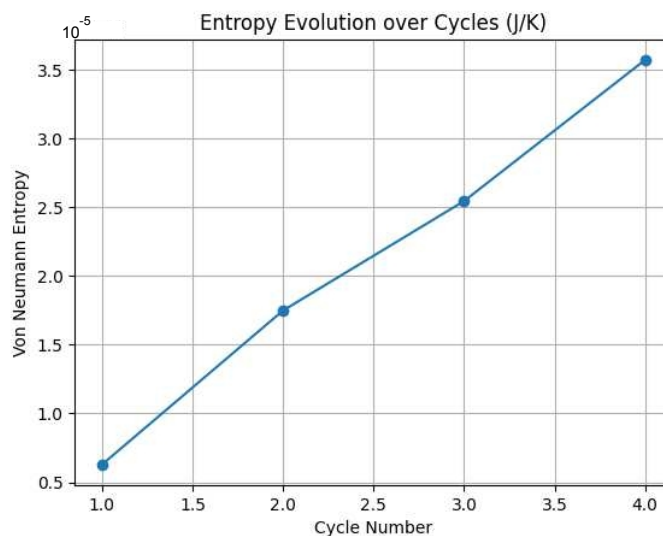


Figure 3. Variation of system von Neumann entropy throughout the quantum Stirling cycles. The energy and the entropy, both quantities exhibit periodic behaviors, offering insights into the engine's thermodynamic processes.

1.4.5. Linear Decoherence in Quantum Stirling Cycles

In our quantum simulations, a linear decrease in coherence over the cycles was observed. This behavior aligns with the phenomenon of decoherence in quantum systems interacting with an environment. Quantum coherence is defined by the off-diagonal elements of the density matrix, and it represents quantum superpositions. Maintaining coherence is crucial for quantum operations as it encapsulates the principle of superposition. However, decoherence arises due to system–environment interactions, leading to a loss of quantum information. This does not imply energy dissipation but indicates a transition from a coherent superposition to a mixture.

The linear decay observed in Figure 4 suggests consistent and uniform interactions or perturbations acting on the system throughout cycles, leading to a steady loss of coherence.

The rate of decoherence can provide insights into system robustness and the efficacy of quantum operations. For practical quantum technologies, understanding and mitigating decoherence is crucial to ensure reliable performance.

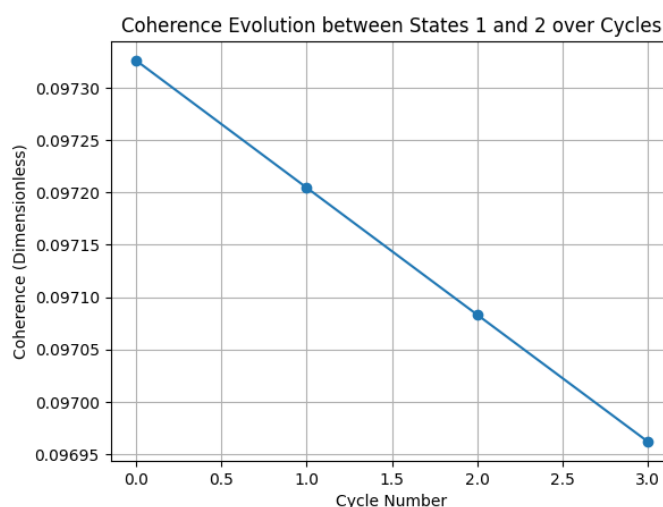


Figure 4. Decay of quantum coherence over the cycles in the quantum Stirling engine. The linear decrease in coherence over time highlights consistent system–environment interactions leading to decoherence.

1.5. Thrust Based on the Gradient in the Refractive Index of a Material

In this section, we explore the theoretical basis for utilizing quantum entanglement to generate thrust within a material medium, particularly using gradients of free energy, as suggested by our Equation (2). It needs to be emphasised that at this point that this idea is still entirely hypothetical and has not been supported by any commonly used equations or experimental data. Here, we investigate the prospect of inducing a gradient in a material's refractive index by the use of entangled photon pairs, so producing a net force on a device. Analog to the instances on hydrophobic surfaces, where water droplets appear to be able to defy gravity and go in unexpected directions, we investigate the feasibility of producing propulsion in a material medium [33–37]. In the same way that the hydrophobic effect uses surface contacts to drive motion with gradients of free energy, our theory takes into account the application of quantum entanglement to control a material's refractive index with the goal of applying a net force to an apparatus. Recent studies, such as those by Porcelli and Filho (2019), have shown that anomalous thrust forces can be measured in resonant microwave cavities. This research highlights the potential role of quantum entanglement in creating force over distances, suggesting a link between microscale quantum phenomena and macroscale effects. However, it is important to note that these findings are preliminary and do not directly validate our theoretical model [38]. Additionally, advances in understanding quantum entanglement, as demonstrated by Erhard, Krenn, and Zeilinger (2019), provide a broader context for our investigation into manipulating material properties, such as the refractive index, through entanglement. These studies contribute to the theoretical foundation of our work, even though direct experimental evidence in this specific application is still lacking [39]. Moreover, experiments like those conducted by Julsgaard, Kozhokin, and Polzik (2001) have successfully entangled macroscopic objects, offering insights into the feasibility of applying quantum entanglement to larger systems [40]. While these experiments do not specifically address thrust generation, they underscore the potential of quantum entanglement in macroscopic applications [40].

We propose a theoretical exploration aimed at investigating the potential implications of quantum entanglement on classical mechanics. This approach is speculative and seeks to identify any theoretical frameworks or models where concepts from quantum mechanics, particularly entanglement, might provide new insights or perspectives within the classical paradigm. We recognize the fundamental differences between classical and quantum mechanics and approach this exploration with an aim to bridge conceptual gaps while adhering to the established principles of both fields.

Let us consider E_{qe} as the energy associated with quantum entanglement. This could be a function of the entanglement entropy S_{ent} and a constant α that characterizes the strength of entanglement (see, e.g., Refs. [41,42]):

$$E_{qe} = \alpha \cdot S_{ent}. \quad (41)$$

The entanglement entropy, a measure of quantum entanglement in a system, might be represented as $S_{ent} = -\sum_i p_i \log(p_i)$, where p_i are the probabilities of the quantum states. For example, in the case of the EM-Drive, the energy contribution from the microwave cavity, E_{mw} , could be related to the cavity's resonant frequency ν and photon number N :

$$E_{mw} = h \cdot \nu \cdot N. \quad (42)$$

This energy might interact with E_{qe} to produce a measurable force. The total energy of the system could be the sum of classical and quantum contributions:

$$E_{total} = E_{classical} + E_{qe} + E_{mw}. \quad (43)$$

The free energy term F could be expanded to include quantum entanglement contributions, such as $F = F(E_{total})$. This could be modeled as a function of both classical free energy and entanglement energy. The modified equation of motion would become:

$$m \frac{\partial v}{\partial t} = -m \frac{\partial \Phi}{\partial r} - \frac{\partial}{\partial r} \left(\frac{J^2}{2I} - \omega \cdot J - F - \alpha \cdot E_{qe} \right). \quad (44)$$

Here, α is a scaling factor for the entanglement energy contribution, and E_{qe} represents the quantum entanglement energy, which could be a function of entanglement entropy and other quantum variables. The modified free energy term F_{total} now encapsulates both the classical free energy and the quantum entanglement energy, acknowledging the potential influence of quantum effects on the system's dynamics.

The quantum mechanical version of the equation is derived by modifying the Hamiltonian in the Schrödinger equation to include the effects of quantum entanglement. The modified Schrödinger equation is:

$$i\hbar \frac{\partial \Psi(\mathbf{r}, t)}{\partial t} = \left[-\frac{\hbar^2}{2m} \nabla^2 + V(\mathbf{r}) + \mathcal{J}(\mathbf{r}, \mathbf{J}, \boldsymbol{\omega}, F) + \hat{E}_{qe}(\mathbf{r}, t) \right] \Psi(\mathbf{r}, t). \quad (45)$$

In this equation, $\Psi(\mathbf{r}, t)$ is the wave function of the system, m is the mass of the particle, $V(\mathbf{r})$ is the external potential, \mathcal{J} represents the thermomechanical and informational aspects, and \hat{E}_{qe} is the operator for quantum entanglement energy.

In conceptualizing the behavior of entangled photon states within a material medium, we might draw an analogy to the movement of macroscopic droplets driven by energy gradients. However, it is important to distinguish the underlying mechanisms. While the motion of droplets can be influenced by classical forces such as surface tension gradients, the dynamics of entangled photons are governed by quantum mechanical principles and interactions with the medium at a microscopic level. Additionally, considering the potential effects of surface free energy gradients, it is worth exploring how such gradients could influence particles with mass, thereby extending our analogy to encompass a broader range of physical phenomena. This approach aims to bridge understanding from the macroscopic, classical world to the subtler, quantum nature of light and its interactions within different environments. We might imagine the motion of entangled photon states within a material medium, just as the movement of these droplets is caused by energy gradients.

This change of focus allows us to better understand the quantum mechanical foundations of force and motion, moving from macroscopic hydrophobic surfaces to the microscopic interactions of photons. So, we now look at how the gradient of spatial wave functions and the laws of quantum entanglement can be used to theoretically develop a new kind of propulsion that bridges the gap between quantum and classical physics. It is important to keep in mind that the definition of force in the context of quantum physics differs from its classical meaning. Here, we investigate how to create motion through the gradient in free energy with the theoretical underpinnings of quantum mechanics. We consider the term

$$S_{ent} = -\alpha \sum_k \lambda_k \log \lambda_k,$$

where λ_k are the eigenvalues of the reduced density matrix ρ_A of a subsystem A , representing the probabilities of the quantum states. This term captures the essence of quantum entanglement in a measurable and computable format.

By calculating the gradient ∇S_{ent} , we aim to bridge the gap between the microscopic quantum world and its macroscopic implications. This approach leads us to a modified force equation:

$$\mathbf{F} = -\nabla (E_{classical} + \alpha (-\text{Tr}(\rho_A \log \rho_A)) + h\nu N).$$

Here, the gradient of the entanglement entropy term $-\alpha \sum_k (\log \lambda_k + 1) \nabla \lambda_k$ is incorporated, synthesizing quantum entanglement with classical force dynamics.

The specific experimental setup and application in question will determine the exact form of the equations and the technique employed to control the entangled photons. There are various researchers working on the use of quantum entanglement for propulsion and other novel applications [43–46], including theoretical physicists such as Avi Loeb [47], Igor Pikovski [48], and Mark Kasevich [49]. The use of the quantum vacuum for propulsion is being developed by NASA [50]. A notable advancement was made by Fickler et al. [51], who proposed a method for encoding information into spatial modes of photons, a significant step forward in quantum information science. This concept is complemented by the work of Mair et al. [52], who demonstrated entanglement involving spatial modes of electromagnetic fields, thereby enhancing the potential for quantum information applications. Further expanding on this theme, Altuzarra et al. [53] explored how polarization-entangled photon pairs interact with plasmonic structures. Their findings are critical in understanding quantum gating and plasmon–photon conversion, crucial aspects of quantum optics. Additionally, Brainis [54] developed a generalized principle for the propagation of entangled photons in position space. This principle is particularly relevant to state shaping and spatial entanglement swapping, offering new avenues for manipulating quantum states. Lastly, the groundbreaking work of Togan et al. [55] reported the successful quantum entanglement between a single optical photon and a solid-state qubit, an essential building block for quantum optical networks.

Self-Propelled EM Device with Metamaterials

To date, it has been challenging to produce macroscopic forces that can effectively propel spacecraft due to the limitations of material technology. However, recent advancements in the field of metamaterials provide new possibilities for creating enormous gradients of free energy [29,56–61] that might be utilized for propulsion purposes. But before they can be used successfully for this purpose, further research and development are required as the practical application of such materials is still in its inception. While the breadth and size of such propulsion systems are currently constrained, present technology enables the production of CubeSats that can be propelled utilizing already-in-use systems and technologies. Therefore, additional research and development in the field of innovative materials and propulsion technology are critical.

The force on the dipole moment is given by (see, e.g., Ref. [62]):

$$\mathbf{F} = \frac{1}{c^2} \left[\mathbf{p} \cdot \nabla \mathbf{E} + \frac{\partial \mathbf{p}}{\partial t} \times \mathbf{B} \right], \quad (46)$$

where \mathbf{p} is the dipole moment. This equation represents the Lorentz force acting on the dipole moment due to the gradient of the electric field and the time derivative of the magnetic field. It takes into account the interaction between the dipole moment and the electromagnetic field, resulting in a net force on the dipole.

Equation (46) for the force exerted on a dipole moment due to an electromagnetic wave can be modified. We can write the dipole moment as $\mathbf{p} = \boldsymbol{\alpha} \cdot \mathbf{E}$, where $\boldsymbol{\alpha}$ is the polarizability tensor. Next, we can expand the polarizability tensor as:

$$\boldsymbol{\alpha} = \epsilon_0 (\chi^{(1)} + \chi^{(2)} \cdot \mathbf{E} + \chi^{(3)} \cdot \mathbf{E}^2 + \dots), \quad (47)$$

where $\chi^{(1)}$ is the linear susceptibility tensor, $\chi^{(2)}$ is the second-order susceptibility tensor, and $\chi^{(3)}$ is the third-order susceptibility tensor. We can neglect higher-order terms in the expansion for small electric fields. Hence, we have:

$$\mathbf{p} = \epsilon_0 \left(\chi^{(1)} \mathbf{E} + \chi^{(3)} |\mathbf{E}|^2 \mathbf{E} \right). \quad (48)$$

Note that, while the second-order susceptibility tensor is neglected in Equation (48) under the assumption of a small electric field limit, the third-order susceptibility tensor is

included because it remains significant even for weak electric fields. Now, we can substitute Equation (48) into Equation (46):

$$\mathbf{F} = \frac{1}{c^2} \left[\epsilon_0 \left(\chi^{(1)} \mathbf{E} + \chi^{(3)} |\mathbf{E}|^2 \mathbf{E} \right) \cdot \nabla \mathbf{E} + \frac{\partial \epsilon_0 \left(\chi^{(1)} \mathbf{E} + \chi^{(3)} |\mathbf{E}|^2 \mathbf{E} \right)}{\partial t} \times \mathbf{B} \right]. \quad (49)$$

The term $(\epsilon_0 (\chi^{(1)} \mathbf{E} + \chi^{(3)} |\mathbf{E}|^2 \mathbf{E}) \cdot \nabla \mathbf{E})$ represents the gradient force or gradient pressure. It arises from the interaction between the spatial variation of the electric field (as captured by $\nabla \mathbf{E}$) and the polarization of the material (described by $\chi^{(1)} \mathbf{E}$ and $\chi^{(3)} |\mathbf{E}|^2 \mathbf{E}$). The gradient force tends to push or pull the material particles or dipoles in the direction of the electric field gradient; the term $(\frac{\partial \epsilon_0 (\chi^{(1)} \mathbf{E} + \chi^{(3)} |\mathbf{E}|^2 \mathbf{E})}{\partial t} \times \mathbf{B})$ represents the radiation pressure or time-varying electromagnetic momentum. It arises from the time variation of the electric field (as captured by $\frac{\partial}{\partial t} (\chi^{(1)} \mathbf{E} + \chi^{(3)} |\mathbf{E}|^2 \mathbf{E})$) and its cross product with the magnetic field \mathbf{B} . The radiation pressure results in a transfer of momentum from the electromagnetic field to the material, causing it to experience a force.

Overall, Equation (49) combines the effects of the gradient force, which depends on the spatial variation of the electric field, and the radiation pressure, which arises from the time variation of the electric field and its interaction with the magnetic field. These phenomena play crucial roles in the interaction between electromagnetic fields and materials, particularly in the context of metamaterials and their response to electromagnetic waves. This equation represents the force acting on the dipole moment in terms of the electric field \mathbf{E} and its spatial and temporal derivatives, as well as the material properties characterized by the susceptibility tensors $\chi^{(1)}$ and $\chi^{(3)}$.

It is significant to note that Equation (49), which assumes the complete conversion of electromagnetic energy to kinetic energy, gives an upper constraint on the thrust that may be created. There are several processes that can generate micro-newtons of thrust in the framework of the equations given above for metamaterials. One such process is the use of plasmonic metamaterials, which are composed of metallic nanoparticles arranged in a specific pattern to manipulate light at the nanoscale. When these materials are illuminated by light, they generate plasmons, which are collective oscillations of electrons. The plasmons can induce forces on the nanoparticles, which can result in a net thrust on the material.

Another process is the use of optomechanical metamaterials, which are composed of mechanical resonators coupled to optical cavities. When light is injected into the cavity, it can interact with the mechanical resonators, inducing mechanical motion. This motion can generate a net thrust on the material.

Both of these processes involve the manipulation of light at the nanoscale to induce forces on metamaterials, which can result in micro-newtons of thrust.

It is possible to imagine a scenario where a pulsed electromagnetic wave traverses a metamaterial and gains intensity, leading to an amplification of thrust. This could potentially occur if the metamaterial is designed to have nonlinear properties, such as a high third-order susceptibility $\chi^{(3)}$ [63,64]). When an intense pulsed electromagnetic wave interacts with such a material, it can induce a nonlinear polarization response that can lead to an amplification of the electromagnetic field inside the material.

If we assume a typical metamaterial with a linear susceptibility of the order of 0.1 and a third-order susceptibility on the order of 10^{-8} , and a pulsed electromagnetic wave with an intensity on the order of 10^{12} W/m², we can estimate the thrust to be on the order of nano-newtons to micro-newtons. However, this is a very rough estimate, and the actual thrust generated will depend on the specific properties of the metamaterial and the pulsed electromagnetic wave.

There have been several studies on the use of metamaterials for propulsion. One notable example is the work by Alu et al. [65], which proposed a metamaterial-based device capable of generating thrust by exploiting the nonlinear response of the material to an incident electromagnetic wave. The device consisted of a rectangular array of metallic split-ring resonators (SRRs) with a nonlinear material in the gaps between the SRRs. When an intense pulsed electromagnetic wave was incident on the device, the nonlinear material generated harmonics at frequencies different from the incident frequency, which in turn generated a net force on the device due to the asymmetric radiation of the harmonics. The authors estimated that the device could generate a thrust on the order of micro-newtons.

Coulais et al. [66] demonstrated the possibility of breaking reciprocity in static systems, enabling mechanical metamaterials to exhibit nonreciprocal behavior.

Another example is the work by Mihai et al. [67], which proposed a metamaterial-based device consisting of an array of cylindrical pillars made of a non-linear material. When an incident electromagnetic wave was incident on the device, the nonlinear material generated harmonics at frequencies different from the incident frequency, which in turn generated a net force on the device due to the asymmetric radiation of the harmonics. The authors demonstrated experimentally that the device could generate a thrust of the order of micro-newtons.

2. Conclusions

In conclusion, this article explores various methods to enhance engine efficiency, considering the limitations imposed by the laws of thermodynamics. The use of nanomaterials and surface engineering capable of harnessing entropy-gradient forces is discussed, highlighting their potential to generate useful work by converting random thermal motion into directed motion. Additionally, the concept of information burning engines, which extract energy from information processing, is discussed in the framework of [9], particularly engines fueled by entanglement, discussing theoretical proposals for quantum Stirling engines and entropy gradient engines. These engines are based on the exploitation of entanglement to extract work from heat baths, showcasing the potential of quantum principles in enhancing engine performance. There is a range of innovative approaches that could contribute to the development of more efficient and sustainable engines, pushing the boundaries of current engine technologies and exploring new frontiers in energy production for sustainable societies.

Funding: This research received no external funding

Institutional Review Board Statement: Not applicable.

Informed Consent Statement: Not applicable.

Data Availability Statement: The data supporting the findings of this study are openly available on GitHub at https://github.com/mjgpinheiro/Physics_models/blob/main/Quantum_Otto_Cycle_Simulator2.ipynb. This data set was generated during the current study and is freely available for review and further analysis.

Acknowledgments: I would like to express my sincere gratitude to Genito Maure, Dinelsa Machaieie, Volodymyr Valentyn Chernysh, and Marina Yuri Kotchkareva for their valuable insights and comments shared during a talk presented at the University Eduardo Mondlane, Maputo, Mozambique, in October 2022. Their contributions have greatly enriched this research project.

Conflicts of Interest: The author declares no conflicts of interest.

References

1. Gulfam, R.; Chen, Y. Recent Growth of Wettability Gradient Surfaces: A Review. *Research* **2022**, *2022*, 9873075. [CrossRef]
2. Bakli, C.; Perumanath, S.; Chakraborty, S. Nanoscale Thermofluidics. *Nanoscale* **2017**, *9*, 12509–12515. [CrossRef]
3. Parrondo, J.M.R.; Horowitz, J.M.; Sagawa, T. Thermodynamics of information. *Nat. Phys.* **2015**, *11*, 131–139. [CrossRef]
4. Toyabe, S.; Sagawa, T.; Ueda, M.; Muneyuki, E.; Sano, M. Experimental demonstration of information-to-energy conversion and validation of the generalized Jarzynski equality. *Nat. Phys.* **2010**, *6*, 988–992. [CrossRef]

5. Quan, H.T.; Liu, Y.X.; Sun, C.P.; Nori, F. Quantum thermodynamic cycles and quantum heat engines. *Phys. Rev. E* **2007**, *76*, 031105. [CrossRef]
6. Gelbwaser-Klimovsky, D.; Niedenzu, W.; Kurizki, G. Quantum thermodynamics: A dynamical viewpoint. *Adv. At. Mol. Opt. Phys.* **2015**, *64*, 329–407. [CrossRef]
7. Rossnagel, J.; Abah, O.; Schmidt-Kaler, F.; Singer, K.; Lutz, E. Nanoscale Heat Engine Beyond the Carnot Limit. *Phys. Rev. Lett.* **2014**, *112*, 030602. [CrossRef] [PubMed]
8. Uzdin, R.; Levy, A.; Kosloff, R. Equivalence of Quantum Heat Machines, and Quantum-Thermodynamic Signatures. *Phys. Rev. X* **2015**, *5*, 031044. [CrossRef]
9. Pinheiro, M.J. Ergotropic Dynamics: Contribution for an Extended Particle Dynamics. In *Rhythmic Advantages in Big Data and Machine Learning: Studies in Rhythm Engineering*; Bandyopadhyay, A., Ray, K. Eds.; Springer: Singapore, 2022. [CrossRef]
10. Pinheiro, M.J.; Pinheiro, M.R.A. Reassessment of the Concept of Momentum in Econophysics. *Eur. J. Appl. Phys.* **2021**, *3*, 25–35. [CrossRef]
11. Piccitto, G.; Campisi, M.; Rossini, D. The Ising critical quantum Otto engine. *New J. Phys.* **2022**, *24*, 103023. [CrossRef]
12. Deffner, S.; Campbell, S. Quantum Thermodynamics. *Morgan Claypool Publ.* **2019**, *10*, 2053–2571. [CrossRef]
13. Saha, T.K.; Lucero, J.N.E.; Ehrich, J.; Sivak, D.A.; Bechhoefer, J. Maximizing power and velocity of an information engine. *Proc. Natl. Acad. Sci. USA* **2021**, *118*, e2023356118. [CrossRef] [PubMed]
14. Von Neumann, J. *Mathematical Foundations of Quantum Mechanics*; Princeton University Press: Princeton, NJ, USA, 1955.
15. Greiner, W.; Neise, L.; Stöcker, H. *Thermodynamics and Statistical Mechanics*; Springer: Berlin/Heidelberg, Germany, 1995.
16. Nielsen, M.A.; Chuang, I.L. *Quantum Computation and Quantum Information*; Cambridge University Press: Cambridge, UK, 2000.
17. Callen, H.B. *Thermodynamics and an Introduction to Thermostatistics*, 2nd ed.; Wiley: Hoboken, NJ, USA, 1985.
18. Kosloff, R.; Rezek, Y. The Quantum Harmonic Otto Cycle. *Entropy* **2017**, *19*, 136. [CrossRef]
19. Klatzow, J.; Becker, J.N.; Ledingham, P.M.; Weinzetl, C.; Kaczmarek, K.T.; Saunders, D.J.; Nunn, J.; Walmsley, I.A.; Uzdin, R.; Poem, E. Experimental Demonstration of Quantum Effects in the Operation of Microscopic Heat Engines. *Phys. Rev. Lett.* **2019**, *122*, 110601. [CrossRef]
20. Peterson, J.P.S.; Batalhão, T.B.; Herrera, M.; Souza, A.M.; Sarthour, R.S.; Oliveira, I.S.; Serra, R.M. Experimental Characterization of a Spin Quantum Heat Engine. *Phys. Rev. Lett.* **2019**, *123*, 240601. [CrossRef] [PubMed]
21. Alicki, R.; Kosloff, R. Introduction to Quantum Thermodynamics: History and Prospects. In *Thermodynamics in the Quantum Regime*; Springer: Cham, Switzerland, 2019; pp. 1–33. [CrossRef]
22. Quan, H.T.; Wang, Y.D.; Liu, Y.X.; Sun, C.P.; Nori, F. Maxwell's Demon Assisted Thermodynamic Cycle in Superconducting Quantum Circuits. *Phys. Rev. Lett.* **2009**, *103*, 090402. [CrossRef] [PubMed]
23. Park, J.J.; Kim, K.H.; Sagawa, T.; Kim, S.W. Heat engine driven by purely quantum information. *Phys. Rev. Lett.* **2013**, *111*, 230402. [CrossRef]
24. Özdemir, A.T.; Müstecaplıoğlu, Ö.E. Quantum thermodynamics and quantum coherence engines. *Turk. J. Phys.* **2020**, *44*, 404–436.
25. Scovil, H.E.D.; Schulz-DuBois, E.O. Three-Level Masers as Heat Engines. *Phys. Rev. Lett.* **1959**, *2*, 262–263. <https://link.aps.org/doi/10.1103/PhysRevLett.2.262>. [CrossRef]
26. Abah, O.; Kosloff, R. Performance of quantum heat engines and refrigerators. *Europhys. Lett.* **2014**, *106*, 20001. [CrossRef]
27. Abah, O.; Kosloff, R. Efficiency of heat engines coupled to nonequilibrium reservoirs. *Entropy* **2015**, *17*, 5744–5764. [CrossRef]
28. Abah, O.; Kosloff, R. Thermodynamic efficiency and energy cost of correlations. *New J. Phys.* **2013**, *15*, 105012.
29. Soukoulis, C.; Wegener, M. Past achievements and future challenges in the development of three-dimensional photonic metamaterials. *Nat. Photon* **2011**, *5*, 523–530. [CrossRef]
30. Polzik, E.S.; Ye, J. Entanglement and spin squeezing in a network of distant optical lattice clocks. *Phys. Rev. A* **2016**, *93*, 021404(R). [CrossRef]
31. Ebadi, S.; Wang, T.T.; Levine, H.; Keesling, A.; Semeghini, G.; Omran, A.; Bluvstein, D.; Samajdar, R.; Pichler, H.; Ho, W.W.; et al. Quantum phases of matter on a 256-atom programmable quantum simulator. *Nature* **2021**, *595*, 227–232. [CrossRef]
32. Pinheiro, M.J. Quantum Otto Cycle Simulator. Available online: https://github.com/mjgpinheiro/Physics_models/blob/main/Quantum_Otto_Cycle_Simulator2.ipynb (accessed on Oct 27, 2023).
33. Zhu, X.; Wang, H.; Liao, Q.; Yudong, D.; Gu, Y. Experiments and analysis on self-motion behaviors of liquid droplets on gradient surfaces. *Exp. Therm. Fluid Sci.* **2009**, *33*, 947–954. [CrossRef]
34. Sommers, A.; Panth, M.; Eid, K. Self-propelled water droplet movement on a laser-etched radial gradient copper surface. *Appl. Therm. Eng.* **2020**, *173*, 115226. [CrossRef]
35. Tan, X.; Zhu, Y.; Shi, T.; Tang, Z.; Liao, G. Patterned gradient surface for spontaneous droplet transportation and water collection: Simulation and experiment. *J. Micromech. Microeng.* **2016**, *26*, 115009. [CrossRef]
36. Liu, C.; Zhou, J.; Zheng, D.; Wan, Y.; Li, Z. Conversion of Surface Energy and Experimental Investigation on the Self-Motion Behaviors of Liquid Droplets on Gradient Surfaces. *Mater. Sci. Forum* **2011**, *687*, 596–601. [CrossRef]
37. Lv, C.; Chen, C.; Chuang, Y.; Tseng, F.; Yin, Y.; Grey, F.; Zheng, Q. Substrate curvature gradient drives rapid droplet motion. *Phys. Rev. Lett.* **2014**, *113*, 026101. [CrossRef]
38. Porcelli, E.B.; Filho, V.S. On the anomalous forces in microwave cavity-magnetron systems. *J. Eng.* **2019**, *2019*, 7279–7286. [CrossRef]

39. Erhard, M.; Krenn, M.; Zeilinger, A. Advances in high-dimensional quantum entanglement. *Nat. Rev. Phys.* **2019**, *2*, 365–381. [[CrossRef](#)]
40. Julsgaard, B.; Kozhekin, A.; Polzik, E. Experimental long-lived entanglement of two macroscopic objects. *Nature* **2001**, *413*, 400–403. [[CrossRef](#)] [[PubMed](#)]
41. Vedral, V. *Introduction to Quantum Information Science*; Oxford University Press: Oxford, UK, 2014.
42. Horodecki, R.; Horodecki, P.; Horodecki, M.; Horodecki, K. Quantum entanglement. *Rev. Mod. Phys.* **2009**, *81*, 865. [[CrossRef](#)]
43. Rovey, J.L.; Friz, P.D.; Hu, C.; Glascock, M.S.; Yang, X. Plasmonic Force Space Propulsion. *J. Spacecr. Rocket.* **2015**, *52*, 1163–1168. [[CrossRef](#)]
44. Levchenko, I.; Xu, S.; Cherkun, O.; Baranov, O.; Bazaka, K. Plasma meets metamaterials: Three ways to advance space micropropulsion systems. *Adv. Phys. X* **2021**, *6*, 1834452. [[CrossRef](#)]
45. Gao, L.; Lu, B.; Xu, H. Materials and applications of flexible metamaterials and plasmonics. *Sci. Sin. Phys. Mech. Astron.* **2016**, *46*, 044604.
46. Esfandiari, M.; Lalbakhsh, A.; Shehni, P.N.; Jarchi, S.; Ghaffari-Miab, M.; Mahtaj, H.N.; Reisenfeld, S.; Alibakhshikenari, M.; Koziel, S.; Szczepanski, S. Recent and emerging applications of Graphene-based metamaterials in electromagnetics. *Mater. Des.* **2022**, *221*, 110920. [[CrossRef](#)]
47. Loeb, A.; Tselikhovich, M. A Roadmap to Interstellar Flight. *J. Br. Interplanet. Soc.* **2012**, *65*, 40–49.
48. Pikovski, I.; Vanner, M.R.; Aspelmeyer, M.; Kim, M.S.; Brukner, C. Probing Planck-scale physics with quantum optics. *Nat. Phys.* **2012**, *8*, 393–397. [[CrossRef](#)]
49. Kasevich, M. Quantum Control and Measurement for Precision Sensing and Fundamental Physics. *Annu. Rev. Cold Atoms Mol.* **2014**, *2*, 177–200.
50. White, H.; March, P.; Williams, N.; O'Neill, W. Eagleworks Laboratories: Advanced Propulsion Physics Research. In Proceedings of the JANNAF Joint Propulsion Meeting (JSC-CN-25207), Huntsville, AL, USA, 5 December 2011.
51. Fickler, R.; Lapkiewicz, R.; Plick, W.; Krenn, M.; Schaeff, C.; Ramelow, S.; Zeilinger, A. Quantum Entanglement of High Angular Momenta. *Science* **2012**, *338*, 640–643. [[CrossRef](#)]
52. Mair, A.; Vaziri, A.; Weihs, G.; Zeilinger, A. Entanglement of the orbital angular momentum states of photons. *Nature* **2001**, *412*, 313–316. [[CrossRef](#)]
53. Altuzarra, C.; Altuzarra, C.; Vezzoli, S.; Valente, J.; Gao, W.; Soci, C.; Faccio, D.; Couteau, C.; Couteau, C.; Couteau, C. Coherent Perfect Absorption in Metamaterials with Entangled Photons. *ACS Photonics* **2017**, *4*, 2124–2128. [[CrossRef](#)]
54. Brainis, E. Quantum imaging with N-photon states in position space. *Opt. Express* **2011**, *19*, 24228–24240. [[CrossRef](#)] [[PubMed](#)]
55. Togan, E.; Chu, Y.; Trifonov, A.; Jiang, L.; Maze, J.; Childress, L.; Dutt, M.; Sørensen, A.; Hemmer, P.; Zibrov, A.; et al. Quantum entanglement between an optical photon and a solid-state spin qubit. *Nature* **2010**, *466*, 730–734. [[CrossRef](#)] [[PubMed](#)]
56. Liu, X.; Xia, F.; Wang, M.; Liang, J.; Yun, M. Working Mechanism and Progress of Electromagnetic Metamaterial Perfect Absorber. *Photonics* **2023**, *10*, 205. [[CrossRef](#)]
57. Engheta, N.; Ziolkowski, R.W. *Metamaterials: Physics and Engineering Explorations*; John Wiley and Sons: Hoboken, NJ, USA, 2013.
58. Ramos, T.; Kuhn, A.G.; Tino, G.M. Quantum Metrology for Gravity and Inertial Sensors. In *Atomic, Molecular, and Optical Physics Handbook*; Drake, G.W.F., Ed.; Springer: New York, NY, USA, 2018; pp. 1–47.
59. Kaltenbaek, R. Quantum Optics and Quantum Information with Trapped Ions. In *Encyclopedia of Applied High Energy and Particle Physics*; Agarwal, A.K., Dugad, S.K., Eds.; Springer: New York, NY, USA, 2018; pp. 1–30.
60. Marletto, C.; Vedral, V. Gravitationally Induced Entanglement between Two Massive Particles is sufficient Evidence of Quantum Effects in Gravity. *Phys. Rev. Lett.* **2017**, *119*, 240402. [[CrossRef](#)] [[PubMed](#)]
61. Davis, E.W.; Zou, S.; Wauchope, S.J. Entangled Atoms as Propulsion System for CubeSat Payloads. *J. Propuls. Power* **2020**, *36*, 145–155.
62. Jackson, J.D. *Classical Electrodynamics*, 3rd ed.; Wiley: New York, NY, USA, 1998.
63. Paul, T.; Geiselmann, M.; Utikal, T.; Zentgraf, T.; Giessen, H.; Rockstuhl, C.; Lederer, F. Enhanced third harmonic generation using plasmonic metamaterials. In Proceedings of the CLEO/Europe—EQEC 2009—European Conference on Lasers and Electro-Optics and the European Quantum Electronics Conference, Munich, Germany, 14–19 June 2009; p. 1. [[CrossRef](#)]
64. Linnenbank, H.; Linden, S. Second harmonic generation spectroscopy on second harmonic resonant plasmonic metamaterials. *Optica* **2015**, *2*, 698–701. [[CrossRef](#)]
65. Alú, A. *Metamaterial-Based Device Engineering—Andrea Alú*; National Academy of Engineering; Frontiers of Engineering: Reports on Leading-Edge Engineering from the 2015 Symposium; The National Academies Press: Washington, DC, USA, 2016. [[CrossRef](#)]
66. Coulais, C.; Sounas, D.; Alú, A. Static non-reciprocity in mechanical metamaterials. *Nature* **2017**, *542*, 461–464. [[CrossRef](#)] [[PubMed](#)]
67. Mihai, L.; Mihalcea, R.; Tomescu, R.; Paun, C.; Cristea, D. Selective Mid-IR Metamaterial-Based Gas Sensor System: Proof of Concept and Performances Tests. *Nanomaterials* **2022**, *12*, 1009. [[CrossRef](#)] [[PubMed](#)]

Disclaimer/Publisher’s Note: The statements, opinions and data contained in all publications are solely those of the individual author(s) and contributor(s) and not of MDPI and/or the editor(s). MDPI and/or the editor(s) disclaim responsibility for any injury to people or property resulting from any ideas, methods, instructions or products referred to in the content.